PNAS
www.pnas.org

Supplementary Information for

Environmental reservoir dynamics predict global infection patterns and population impacts for the fungal disease white-nose syndrome

Joseph R. Hoyt, Kate E. Langwig, Keping Sun, Katy L. Parise, Aoqiang Li, Yujuan Wang, Xiaobin Huang, Lisa Worledge, Helen Miller, J. Paul White, Heather M. Kaarakka, Jennifer A. Redell, Tamás Görföl, Sándor András Boldogh, Dai Fukui, Muneki Sakuyama, Syuuji Yachimori, Akiyoshi Sato, Munkhnast Dalannast, Ariunbold Jargalsaikhan, Nyambayar Batbayar, Yossi Yovel, Eran Amichai, Ioseb Natradze, Winifred F. Frick, Jeffrey T. Foster, Jiang Feng and A. Marm Kilpatrick

Corresponding Author:
Joseph R Hoyt
Email: hoytjosephr@gmail.com

This PDF file includes:

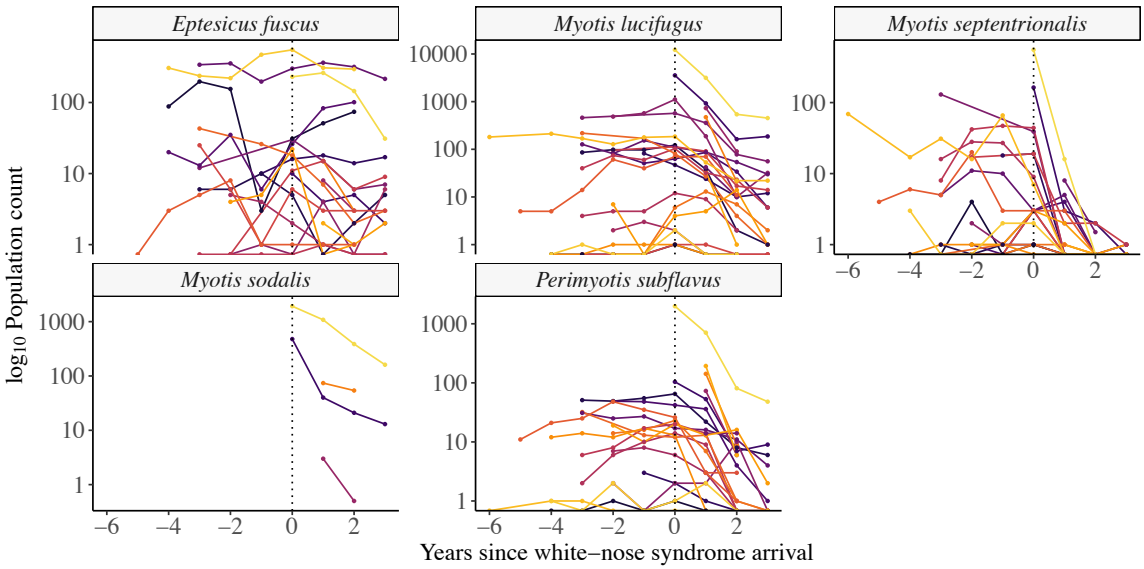

Figure S1. Individual population trajectories for North American bat species. Each panel represents a different species and the lines show an individual population of that species at a site over time which are used to estimate the population growth rates shown in Fig. 1A. The y-axis scale varies among panels and represents the $\log_{10}$ populations size for each species. The x-axis shows the years since the invasion of *P. destructans* with 0 indicating the first year of *P. destructans* invasion into a population and is denoted by a dotted vertical line.

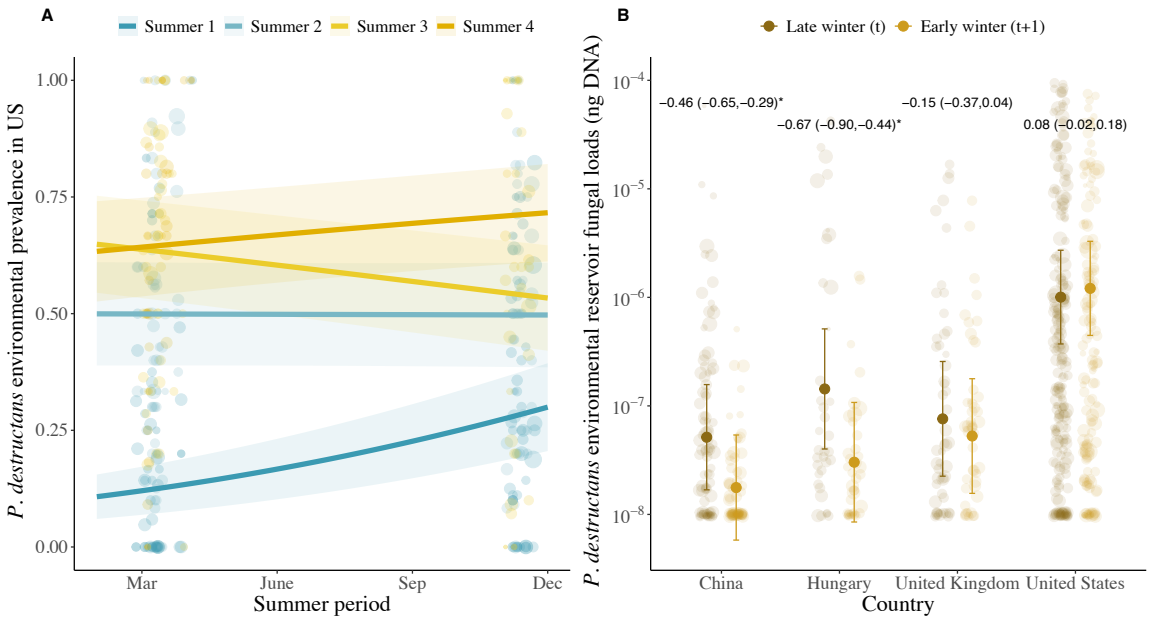

Figure S2. Environmental pathogen reservoir dynamics over the summer. (A) The change in *P. destructans* environmental reservoir prevalence over the summer in the US following the invasion of *P. destructans* into sites (Slope coefficients for the change in *P. destructans* environmental reservoir prevalence over the summers following pathogen invasion (Summer 1: 0.13 ± 0.02 (0.1,0.17); Summer 2: 0 ± 0.02 (-0.03,0.03); Summer 3: -0.05 ± 0.02 (-0.09, 0.04); Summer 4: 0.04 ± 0.03 (-0.02,0.1)). Summer period (1, 2, 3, and 4) indicates the summer between two winter periods since *P. destructans* invasion (e.g. Summer 1 is between the invasion year and year 2 with *P. destructans*; Fig. 2). Transparent points show the raw data at each sampling point. **(B)** The change in fungal loads between late winter (t) and early winter (t+1) sampling across the globe. The coefficients (posterior mean and 95% HDP) above each country represent the seasonal change from spring to autumn for that country and the asterisk (*) indicates whether there was support for the change fungal loads in the environment over summer either increasing or decreasing. Transparent points show the average fungal loads for a sampling type at a site for a given sampling day.

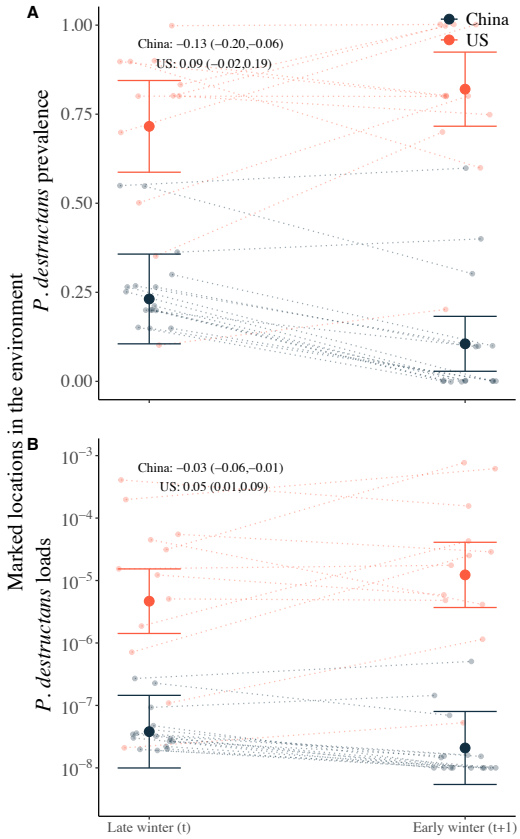

Figure S3. The change in fungal dynamics in the environment over the summer at fixed locations. The change in *P. destructans* **(A)** prevalence and **(B)** fungal loads (log_{10} ng DNA) in the environment at fixed marked locations sampled over time in the US and China. The coefficients represent the monthly change over the summer in fungal prevalence (logit scale) and fungal loads (response scale). For display purposes, points show the fungal **(A)** prevalence and the **(B)** mean fungal loads aggregated across all the sampling stations in a section. The monthly change in prevalence from late winter in year t to early winter in year t+1: China: -0.13 (-0.20,-0.06), US: 0.09 (-0.02,0,19), and the monthly change in fungal loads from late winter t to early winter t+1: China: -0.03 (-0.06,-0.01), US: 0.05 (-0.01,0,09). The dotted lines connect individual locations marked in the environment sampled in late winter (t) and again in early winter (t+1).

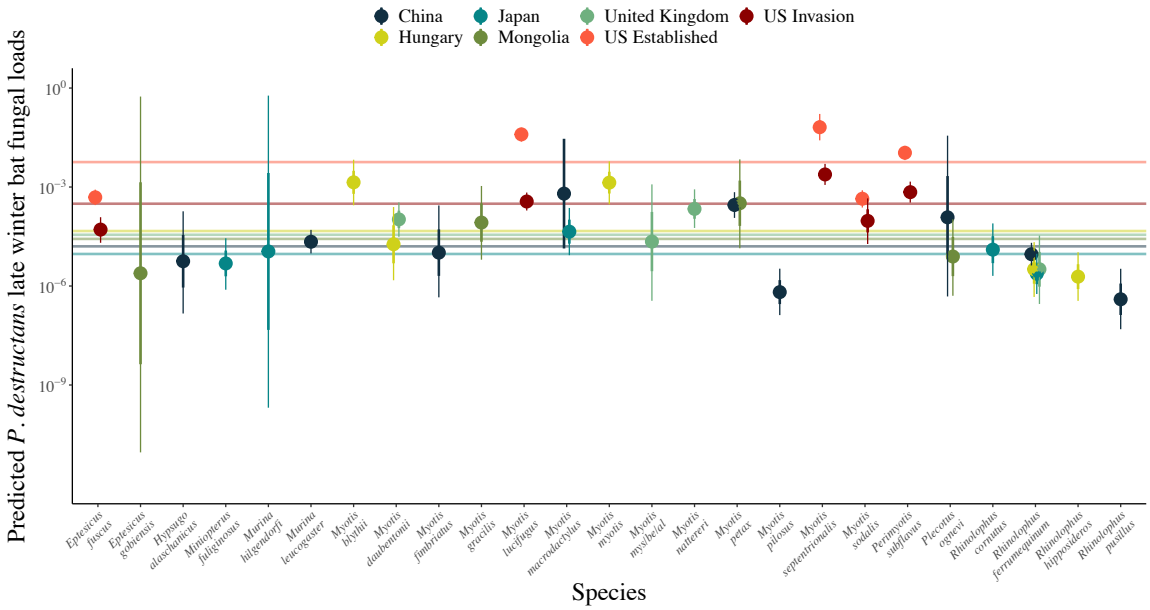

Figure S4. Predicted late winter fungal loads (log_{10} ng DNA) for 25 species of bats across the globe. Points indicate the posterior mean, thick bars indicate ± 1 standard deviation of the posterior mean and thin bars indicate the 95% credible intervals. To account for differences in sampling date among regions we fit a model with fungal loads as our response variable and sampling date interacting with species as our predictor. We then extracted the posterior mean for all species on the same date (March 1st), which is shown above. Species that were sampled in multiple regions are shown with a mean fungal load for each region sampled (e.g. *Rhinolophus ferrumequinum* was sampled in China, Hungary, Japan, and the U.K.). For species in the U.S. we show fungal loads on species during the first year of invasion (dark red points) compared to data from all years following when large mortality occurs (light red points). Regions or species that were sampled at just a single time point were excluded as we could not estimate the over winter change in fungal loads. Solid lines represent the mean across all species sampled in each country at the end of winter as a reference for comparison among species and regions.

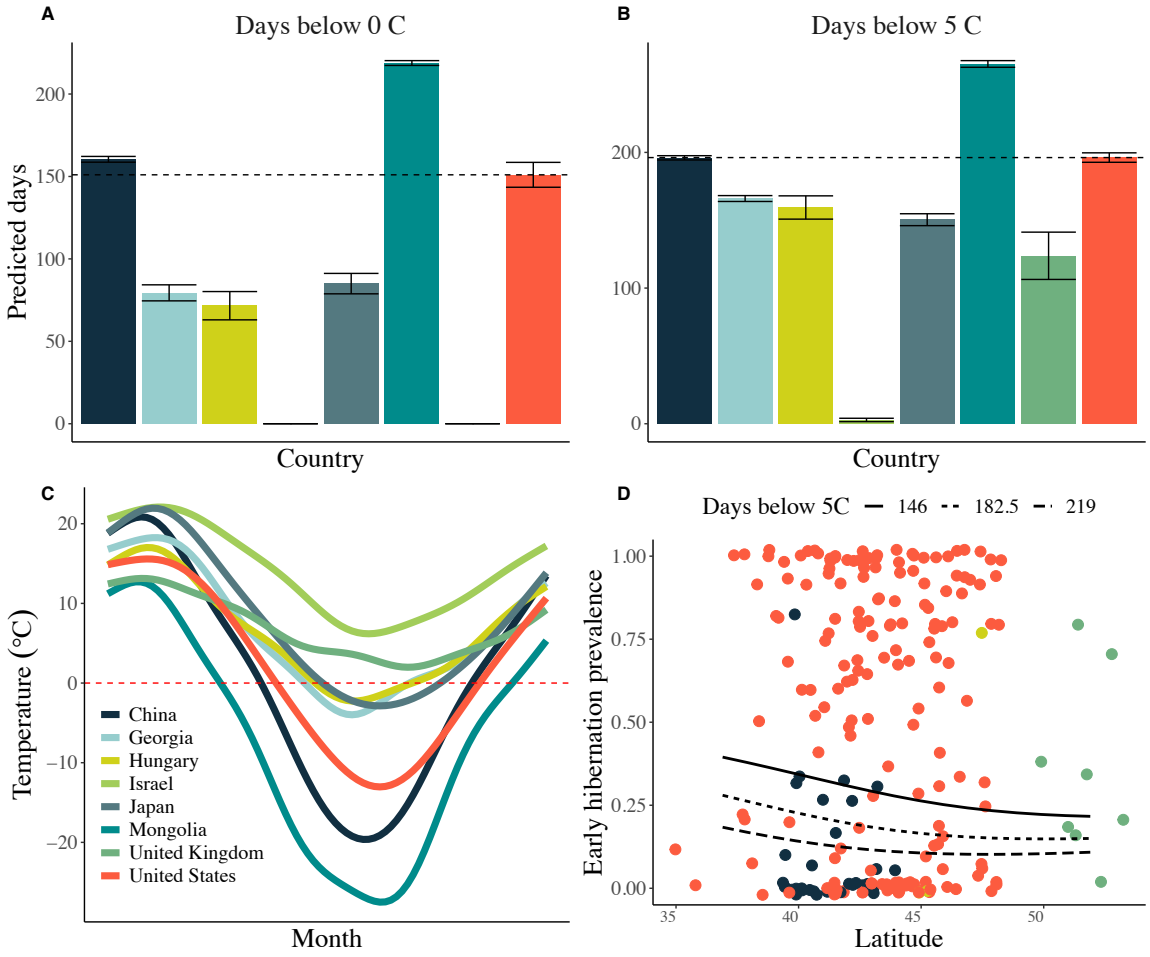

Figure S5. Predicted bat hibernation length as days below 0, and 5 °C and the relationship between latitude and early hibernation bat prevalence. Bar plots show the mean days below 0 **(A)** and 5°C **(B)** for each country between the sampling period (2012–2019) and error bars show the standard error for the mean number of days below a threshold from multiple years. The black dotted line in panels **A** and **B** represents the mean number of days below a predicted temperature for regions sampled in the United States (below 0°C: 151 days; below 5°C: 196 days). Predicted days described in **(A-C)** were calculated from the output of a generalized additive model (GAM) of daily temperature minimums for each country over each year (weather stations 200 km from sites in each country) over a total of 8 years. **(C)** One annual GAM predicted fit to each country with the red line showing the 0°C threshold for comparison purposes. **(D)** The relationship between site latitude, days below 5°C for a region and the early winter bat prevalence estimates for species in those sites. We found no support for a relationship (early hibernation prevalence intercept-4.34 (-10.45, 18.83), latitude slope: -0.07 (-0.34, 0.22), hibernation days slope: -6.23 (-13.37, 0.92)).

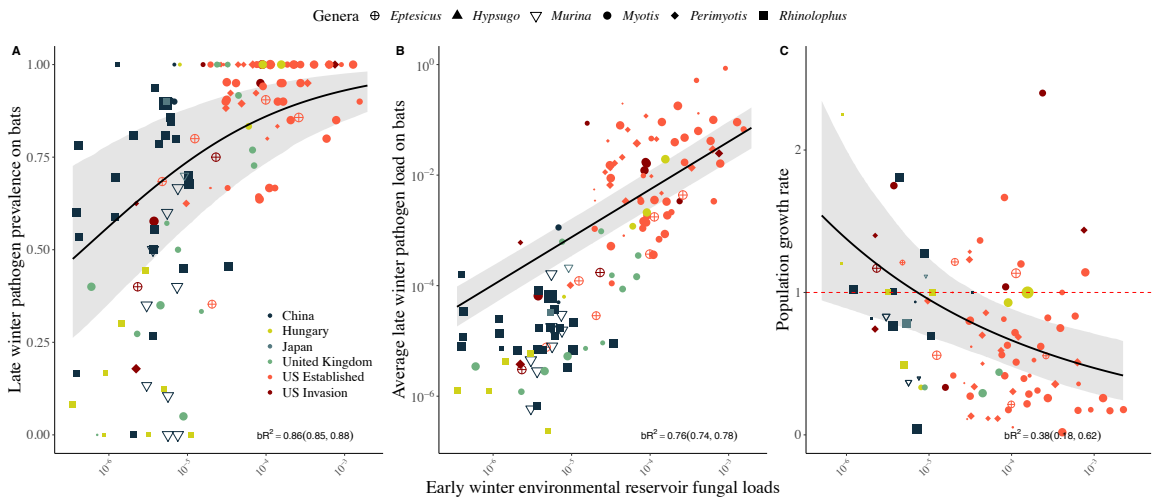

Figure S6. Relationship between late winter *Pseudogymnoascus destructans* prevalence (A), fungal loads (B) and annual population growth rates (C) of bats and fungal loads (log_{10} ng DNA) in the environmental reservoir in early winter. Black lines show the posterior mean and the gray ribbons show 95% credible intervals. The size of the points in each panel represent the sample size from bats **(A & B)** and the environment **(C)** for a species or the substrate sample at a site. The shape indicates the genus of the bat species for each point. **(A & B)** The relationship between late winter bat prevalence and the early winter quantity of *P. destructans* in the environment (within 10 cm of bats) (**A**; intercept: 5.12 (3.48,6.66), slope: 0.81 (0.54,1.08)) and late winter fungal loads on bats and early winter *P. destructans* quantity in the environment (**B**; intercept: 1.20 (0.73,1.68), slope: 0.86 (0.79,0.94)). Each point shows a prevalence estimate or mean fungal load for a species at a site and the contamination of *P. destructans* 10cm around that species at a site. **(C)** The relationship between population growth rates for a bat species at a site and pathogen quantity in the environment 10 cm around that species at a site in early winter (intercept: -1.84 (-2.82, -0.80); slope: -0.36 (-0.56, -0.14)). Each dot shows the fungal load of *P. destructans* in the environment 10cm from around individuals of that species at a site in early winter (x-axis) and the y-axis shows the population growth rate (N_{t+1}/N_t) from the previous late winter, N_t, to the following late winter, N_{t+1}. The horizontal red line indicates population stability.

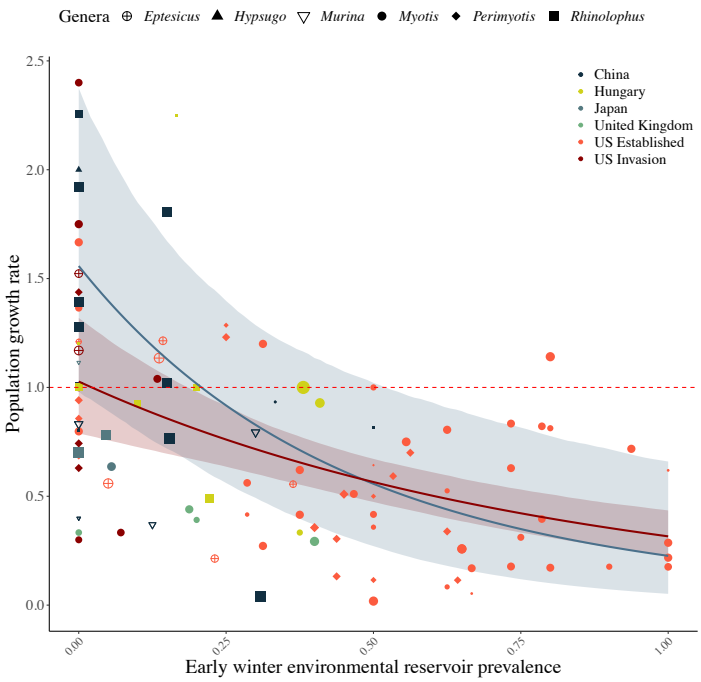

Figure S7. The relationship between bat population growth rates at a site and fungal loads in the environment 10cm around that species at a site in early winter (Eurasia intercept: 0.43 (-0.01,0.86); slope:-2.13 (-3.46,-0.77), North America intercept: 0.02 (-0.24,0.30); slope: -1.18 (-1.69,-0.70)). The line and shaded region indicate the posterior mean and 95% credible intervals for the data fit to bat populations in Eurasia (blue) and North America (red). Each dot shows the prevalence of *P. destructans* in the environment 10 cm from around individuals of that species at a site in early winter (x-axis) and the y-axis shows the population growth rate (N_{t+1}/N_t) from the previous late winter, N_t, to the following late winter, N_{t+1}. The horizontal red line indicates population stability.

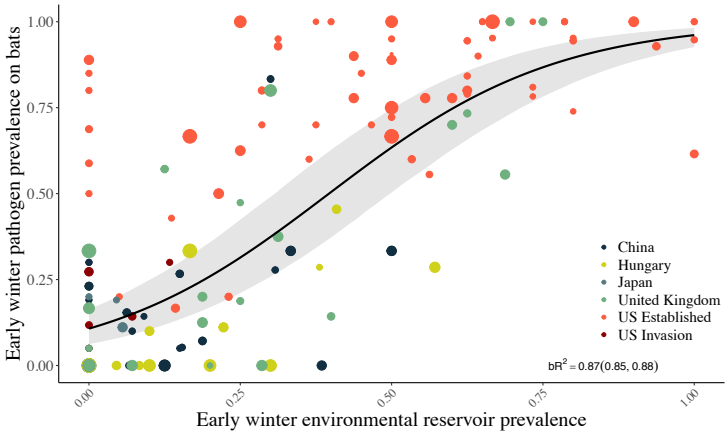

Figure S8. Relationship between *Pseudogymnoascus destructans* prevalence in the environmental reservoir and on bats in early winter. Black lines show the posterior mean and the gray ribbons show 95% credible intervals. The size of the points in each panel represent the sample size of bat species sampled at a site. Each point shows a prevalence estimate for a species at a site and the contamination of *P. destructans* near that species at the same time point (t) (early bat prevalence intercept-2.14 (-2.72, -1.61), early reservoir slope: 5.35 (4.69, 6.05)). bR^2 are Bayesian R^2 values, calculated as the variance of the predicted values divided by the variance of predicted values plus the variance of the errors.

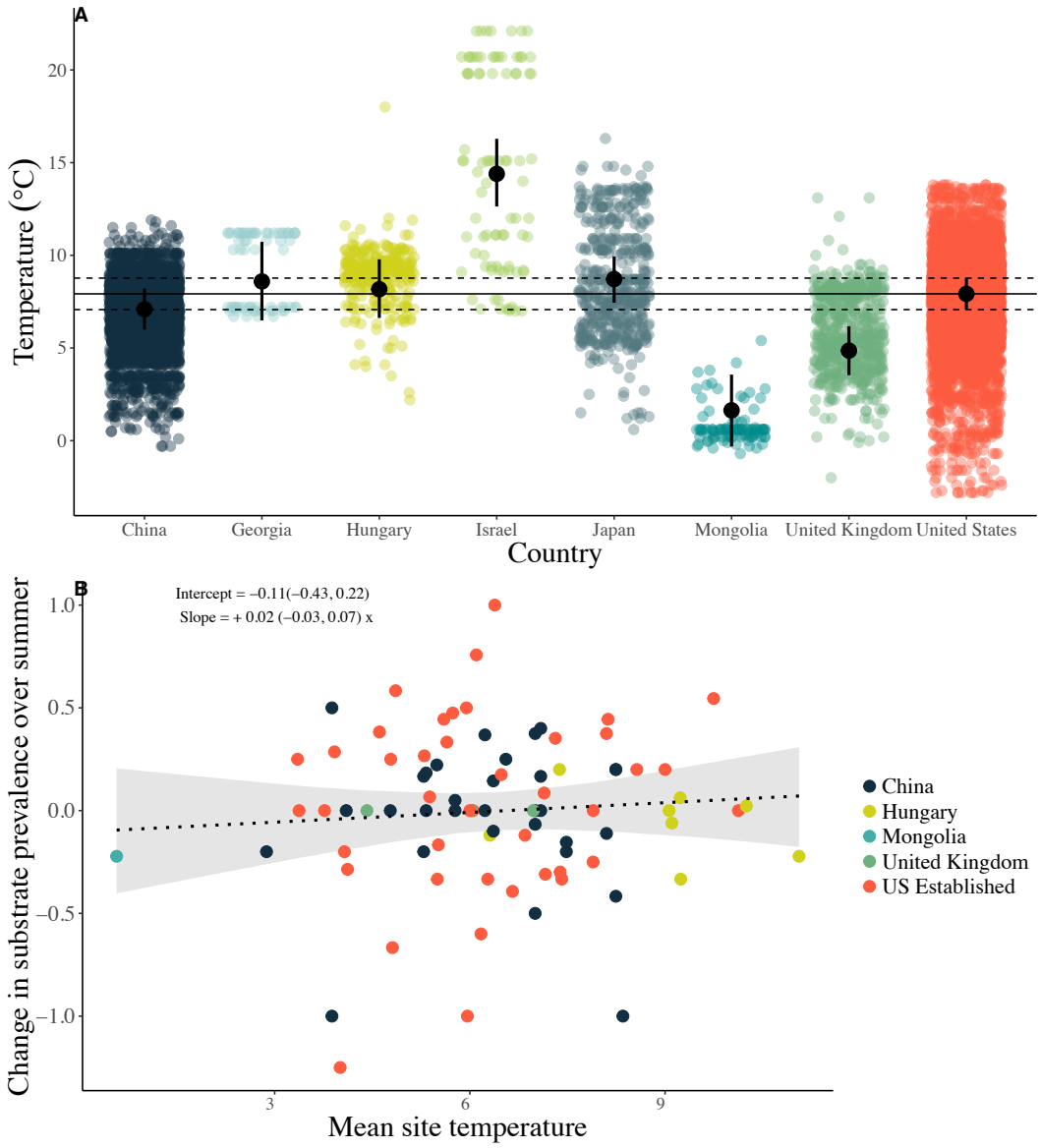

Figure S9. Roosting temperatures of hibernating bats across North America and Eurasia and the relationship between the decay or persistence of *P. destructans* in the environment. **(A)** Points show an individual roosting temperature of bats over the winter by region. Black points show the posterior mean and 95% CI for each region accounting for species and site where the measurement was taken. The solid line shows the posterior mean and the dashed lines represent the 95% credible intervals (7.92 (7.07, 8.77)) for bat roosting temperatures in the United States (Table S18). **(B)** The relationship between the change in *P. destructans* prevalence in the substrate at a site and the mean temperature for the site across the United States, United Kingdom, Hungary, and China. We find no support that within site temperature is mediating the observed decay or persistence of *P. destructans* in the environment over summer periods when bats are absent from sites (change in prevalence intercept: -0.11(-0.43,0.22), mean site temperature slope: 0.22(-0.03,0.07)).

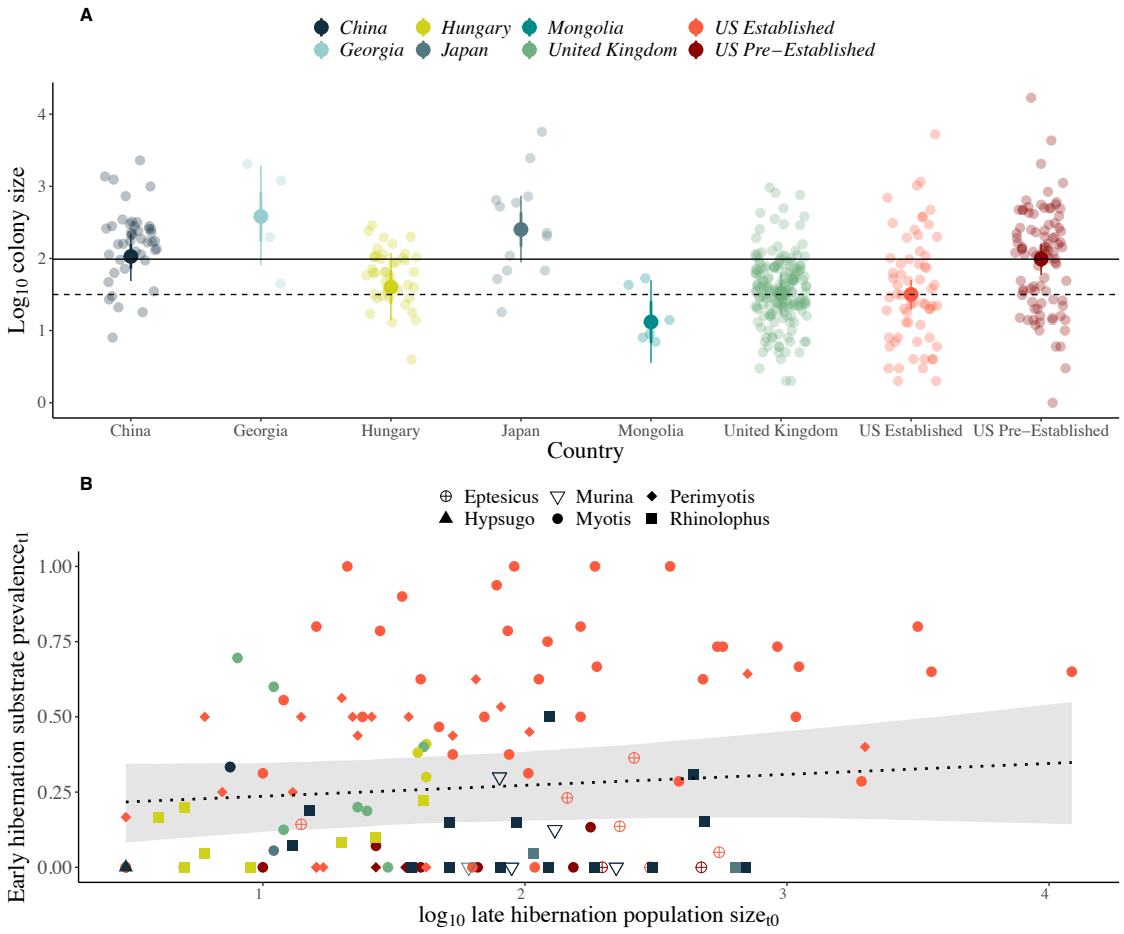

Figure S10. Colony size and the relationship between bat density and environmental reservoir prevalence. (A) The $\log_{10}$ colony size at a site across different regions during late winter. Each transparent point represents a total population count at a site. The larger points indicate the posterior mean and thick bars indicate the standard deviation of the posterior mean and thin bars indicate the 95% credible intervals. Data for the U.S. was separated by colony size before the establishment of *P. destructans* into sites (US Pre-Established) which includes the first year of invasion before population declines have occurred (Fig. 1B) and colony size after the establishment of *P. destructans* into sites when large declines have occurred. The horizontal solid line indicates the mean colony size for bats in the U.S. before white-nose syndrome declines and the dotted line indicates the mean colony sites after declines from white-nose syndrome. **(B)** The relationship between $\log_{10}$ population size during late winter (t) and the early winter pathogen prevalence in the environment around that population the following winter ($_{t+1}$). We found no support for the density of bats influencing the prevalence of *P. destructans* in the environment the following winter (intercept: 0.20 (0.05,0.35), population size slope: 0.04 (-0.03, 0.11)).

Appendix 1. Summary of figures, statistical analyses, and the corresponding results throughout the manuscript.

Figure	Table #	Distribution	Response Variable	Population-effect	Group-effect	Data	Findings
Fig. 1A	S2	Gaussian	Annual Eurasian bat population growth rate	Species	Site	Eurasian	Eurasian Bat species are stable but with variable population growth rates
Fig. 1B	S3	Gaussian	Annual North American bat population growth rate	Species+ Year since pathogen invasion	Site	North American	US bat populations are stable during invasion, but decline in year 2-4 following the invasion of *Pd*
Fig 2A	S4	Binomial	Pathogen detection (0|1) in environment	Date* Type* Year(con.)	Site	North American	Prevalence increases in the environment following invasion across years 1-4
Fig. 2B	S5	Binomial	Pathogen detection (0|1) on bats	Date* Species* Year(cat.)	Site	North American	During pathogen invasion early winter prevalence is lower than during establishment
Fig. S2A	S6	Binomial	Pathogen detection (0|1) in environment	Date* Summer since *P. destructans* invasion	Site+ Type	North American	Substrate prevalence is stable or increasing over most summers in North America
Fig. S2B	S7	Gaussian	Fungal loads in the environment (log10 ng DNA)	Season* Country	Site+ Type+ Year coll.	All data	Fungal loads are stable over the summer in the US and declining in China, Hungary, and the UK
Fig. S3A	In Fig. legend	Binomial	Pathogen detection (0|1) in environment	Date* Country	[station ID]Site	Substrate stations	Fungal prevalence in the environment over the summer are stable or increasing in the US and declining in China
Fig. S3B	In Fig. legend	Gaussian	Fungal loads in the environment (log10 ng DNA)	Date* Country	[station ID] Site	Substrate stations	Fungal loads in the environment over the summer are stable or increasing in the US and declining in China
Fig. 3 panels	S8	Binomial	Pathogen detection (0|1) on bats	Date* Species_ country (US as Invasion Established)	Site	All data	Changes in prevalence on species is similar during the first year of invasion in North America to Eurasia
Fig. 3 panels	S9	Binomial	Pathogen detection (0|1) on bats	Species	Site	Israel and Georgia	Prevalence is low on bats in midwinter in Georgia and Israel

Figure	Table #	Distribution	Response Variable	Population-effect	Group-effect	Data	Findings
Fig. 4A	S10	Binomial	Pathogen detection (0|1) in environment	Date* country (US combined)	Site+Type +Year collected	US, UK, Hungary, China	Substrate prevalence declines over the summer in Eurasia and is stable in North America
Fig. 4B	S11	Binomial	Pathogen detection (0|1) on bats	Date* country (US as Invasion and Established)	Site+ Species	All data	Changes in prevalence on bats is similar during the first year of invasion in North America to bats Eurasia
Fig S4	S12	Gaussian	Fungal loads on bats (log10 ng DNA)	Date*Species country(US as Invasion Established)	Site	All data	Fungal loads on bats in the US during invasion differ from subsequent years and are more similar to Eurasian bats
Fig. S5A	In plot	GAM	Mean daily temperature at weather stations	Country		Climate data	Climate varies among regions sampled but is similar among the US, China
Fig. S5B	In Fig. legend	Gaussian	Change in bat prevalence at a site over winter	Latitude+ Days below 5C	Site+ Species	All data	No relationship between climate and early hibernation prevalence on bats
Fig. 5A	In Fig. legend	Binomial	Pathogen detection (0|1) on bats t+1	Early winter substrate prevalence at t	Site+ Species	All data	Early substrate prevalence predicts late winter bat prevalence
Fig. 5B	In Fig. legend	Gaussian	Fungal loads on bat populations t+1	Early winter substrate prevalence at t	Site+ Species	All data	Early substrate prevalence predicts late winter bat fungal loads
Fig. 5C	In Fig. legend	Gaussian	Annual bat population growth rate	Early winter substrate prevalence at t	Site+ Species	All data	Early substrate prevalence predicts annual population growth rate of bats
Fig. S6A	In Fig. legend	Binomial	Pathogen detection (0|1) on bats t+1	Early winter substrate loads at t	Site+ Species	All data	Early substrate fungal loads predicts late winter bat prevalence
Fig. S6B	In Fig. legend	Gaussian	Fungal loads on bat populations t+1	Early winter substrate loads at t	Site+ Species	All data	Early substrate fungal loads predicts late winter bat fungal loads
Fig. S6C	In Fig. legend	Gaussian	Annual bat population growth rate	Early winter substrate loads at t	Site+ Species	All data	Early substrate fungal loads predicts annual bat population growth rate
Fig. S7	In Fig. legend	Gaussian	Annual bat population growth rate	Early winter substrate prevalence at t*Continent	Site+ Species	Eurasia and N.A. separate	Early substrate prevalence predicts annual population growth rate of bats similarly across the globe

Figure	Table #	Distribution	Response Variable	Population-effect	Group-effect	Data	Findings
Fig. S8	In Fig. legend	Binomial	Early winter bat prevalence t	Early winter substrate prevalence t	Site+ Species	All date	Early substrate prevalence predicts early prevalence on bats
Fig. S9A	S13	Gaussian	Bat roosting temperature	Country	Site+ Species	All data (US Pre-invasion)	Hibernating bat rooting temperatures don't differ between the US and Hungary, China, Georgia, and Japan
Fig. S9B	In Fig. legend	Gaussian	Change in environmental prevalence over the summer	Mean roosting temperature at a site	Site	All data	No relationship between roosting temperatures in a site and the change in environmental prevalence at that site
Fig.S10A	S14	Gaussian	Total colony size	Country (US as Invasion and Established)	Site	All data	Hibernating bat colony size doesn't differ between the US and Hungary, China, and the UK post-decline
Fig. S10B	In Fig. legend	Gaussian	Bat density at a site (t)	Early substrate prevalence at a site (t+1)	Sites+ Species	All data	No relationship between colony size in a site and the early winter environmental prevalence in that site

Table S1. Species and sample sizes across North America, Europe and Asia. Four-five letter codes represent genus and species for each bat species sampled. Sample sizes indicate number of samples collected for each species within a country. Substrate sample size indicates total number of under, near and far samples collected from the hibernacula environment. For population growth rates in Fig. 1A *Myotis blythii* and *Myotis myotis* (MYBLM) were combined since these two species can be difficult to identify from each other while roosting during hibernation and in some years population counts were combined. All analyses examining disease dynamics, these two species were identified and separated. Similarly, *Myotis mystacinus, Myotis brandtii and Myotis alcathoe* (MYMBA) were combined due to difficulties in identifying these species during hibernation and both population and disease data are combined. The column with *P. destructans* detection indicates whether a species or the substrate tested positive in the respective country.

Species	Species graph code	Samples	Country	*P. destructans* detected on
Eptesicus fuscus	EPFU	1286	US	+
Eptesicus gobiensis	EPGO	12	Mongolia	+
Hypsugo alaschanicus	HYAL	85	China	+
Miniopterus fuliginosus	MIFU	104	Japan	+

Species	Species graph code	Samples	Country	*P. destructans* detected on
Miniopterus schreibersii	MISH	22	Georgia	+
Miniopterus schreibersii	MISH	10	Israel	-
Murina hilgendorfi	MUHI	35	Japan	+
Murina leucogaster	MULE	803	China	+
Myotis aurascens	MYAU	9	Mongolia	+
Myotis blythii	MYBL	31	Hungary	+
Myotis blythii/ Myotis myotis	MYBLM		Hungary	+
Myotis capaccinii	MYCA	15	Israel	+
Myotis dasycneme	MYDAS	4	Hungary	+
Myotis daubentonii	MYDAU	13	Hungary	+
Myotis daubentonii	MYDAU	271	UK	+
Myotis emarginatus	MYEM	5	Hungary	+
Myotis fimbriatus	MYFI	17	China	+
Myotis formosus	MYFO	6	China	+
Myotis frater	MYFR	5	China	+
Myotis gracilis	MYGRA	40	Mongolia	+
Myotis lucifugus	MYLU	2373	US	+
Myotis macrodactylus	MYMA	13	China	+
Myotis macrodactylus	MYMA	56	Japan	+
Myotis myotis	MYMYO	81	Hungary	+
Myotis mystacinus/brandtii/alcathoe	MYMBA	31	UK	+
Myotis nattereri	MYNA	3	Hungary	+
Myotis nattereri	MYNA	4	Israel	-
Myotis nattereri	MYNA	204	UK	+
Myotis petax	MYPE	83	China	+
Myotis petax	MYPE	13	Mongolia	+
Myotis pilosus	MYPI	52	China	+
Myotis septentrionalis	MYSE	663	US	+
Myotis sodalis	MYSO	382	US	+
Perimyotis subflavus	PESU	1932	US	+
Plecotus ognevi	PLOG	18	China	+
Plecotus ognevi	PLOG	31	Mongolia	+
Rhinolophus cornutus	RHCO	101	Japan	+

Species	Species graph code	Samples	Country	*P. destructans* detected on
Rhinolophus euryale	RHEU	28	Georgia	-
Rhinolophus euryale	RHEU	10	Israel	-
Rhinolophus ferrumequinum	RHFE	1029	China	+
Rhinolophus ferrumequinum	RHFE	7	Georgia	+
Rhinolophus ferrumequinum	RHFE	65	Hungary	+
Rhinolophus ferrumequinum	RHFE	6	Israel	-
Rhinolophus ferrumequinum	RHFE	198	Japan	+
Rhinolophus ferrumequinum	RHFE	95	UK	+
Rhinolophus hipposideros	RHHI	8	Georgia	-
Rhinolophus hipposideros	RHHI	120	Hungary	+
Rhinolophus hipposideros	RHHI	6	Israel	-
Rhinolophus pusillus	RHPU	25	China	+
Rhinopoma cystops	RHCY	11	Israel	-
Rhinopoma microphyllum	RHMI	14	Israel	-
Rousettus aegyptiacus	ROAE	10	Israel	-
Vespertilio sinensis	VESI	8	China	+
Substrate	SUBSTRATE	2415	China	+
Substrate	SUBSTRATE	857	Hungary	+
Substrate	SUBSTRATE	188	Israel	-
Substrate	SUBSTRATE	634	Japan	+
Substrate	SUBSTRATE	127	Mongolia	+
Substrate	SUBSTRATE	1161	UK	+
Substrate	SUBSTRATE	5530	US	+

Table S2. Coefficients from a Bayesian hierarchical model for population growth rates of species across Europe and Asia. The data were analyzed with a gamma distribution and log link including site as a group level effect and species as a population-level effect (*Myotis nattereri* (MYNA)*, Murina hilgendorfi* (MUHI)*, Rhinolophus cornutus* (RHCO), *Barbastella barbastellus* (BABA)*, Rhinolophus euryale* (RHEU), *Rhinolophus hipposideros* (RHHI), *Miniopterus fuliginosus* (MIFU), *Plecotus auritus* (PLAU), *Myotis blythii & Myotis myotis combined* (MYBLM), *Myotis mystacinus, Myotis brandtii, and Myotis alcathoe combined* (MYMBA), *Myotis emarginatus* (MYEM), *Myotis petax* (MYPE), *Myotis daubentonii* (MYDAU), *Rhinolophus ferrumequinum* (RHFE), *Hypsugo alaschanicus* (HYAL)*, Murina leucogaster* (MULE)). We used the annual population growth rate as the response variable estimated as the change between two population counts. The model is parameterized in relation to the reference level or intercept (MYNA) and each parameter represents the difference from this reference level. Results visualized in Fig. 1A.

	Posterior Mean ± Standard Error (95% CI)
Intercept (MYNA)	1.07 ± 0.07 (0.93,1.22)
Species MUHI	0.29 ± 0.39 (-0.49,1.06)
Species RHCO	0.07 ± 0.38 (-0.7,0.82)
Species BABA	0.01 ± 0.24 (-0.45,0.48)
Species RHEU	0.01 ± 0.39 (-0.76,0.75)
Species RHHI	0.01 ± 0.15 (-0.27,0.3)
Species MIFU	-0.01 ± 0.39 (-0.76,0.74)
Species PLAU	0.01 ± 0.2 (-0.39,0.39)
Species MYBLM	-0.14 ± 0.16 (-0.44,0.18)
Species MYMBA	-0.04 ± 0.2 (-0.42,0.36)
Species MYEM	-0.04 ± 0.29 (-0.6,0.52)
Species MYPE	-0.05 ± 0.19 (-0.42,0.32)
Species MYDAU	-0.12 ± 0.1 (-0.32,0.08)
Species HYAL	-0.11 ± 0.25 (-0.61,0.38)
Species RHFE	-0.11 ± 0.11 (-0.34,0.11)
Species MULE	-0.21 ± 0.14 (-0.48,0.06)

Table S3. Coefficients from a Bayesian hierarchical model for population growth rates of different species in North America in different years since pathogen detection. The data were analyzed with a gaussian distribution including site as a group level effect and species (*Myotis lucifugus* (MYLU), *Eptesicus fuscus* (EPFU), *Myotis septentrionalis* (MYSE)*, Myotis sodalis* (MYSO) and *Perimyotis subflavus* (PESU)) with an additive effect year since first *P. destructans* detection (YSW; years 1–4 as a categorical variable) as population-level effects. We used the annual population growth rate as the response variable estimated as the change between two population counts. The model is parameterized in relation to the reference level or intercept (MYLU: pre-pathogen invasion year 0) and each parameter represents the difference from this reference level, incorporating the effect of species and year since first pathogen detection. Results can be visualized in Fig. 1B.

	Posterior Mean ± Standard Error (95% CI)
Intercept (MYLU)	1.05 ± 0.08 (0.9,1.19)
EPFU	0.17 ± 0.08 (0.02,0.32)
MYSE	-0.05 ± 0.1 (-0.25,0.14)
PESU	0.01 ± 0.08 (-0.14,0.16)
MYSO	-0.07 ± 0.17 (-0.41,0.28)
YSW1	-0.05 ± 0.09 (-0.23,0.13)
YSW2	-0.37 ± 0.09 (-0.55,-0.2)
YSW3	-0.58 ± 0.09 (-0.76,-0.4)
YSW4	-0.32 ± 0.11 (-0.53,-0.1)

Table S4. Coefficients from a Bayesian hierarchical model for changes in pathogen prevalence in North America in the environment in different years since pathogen detection. The data were analyzed with a binomial distribution and logit link including site as a group level effect and date interacting with sample type (samples collected from the substrate under or adjacent to bats (UNDER), samples collected from the substrate 10 cm from a bat (NEAR), and samples collected >2 m from a bat (FAR)) and year since first *P. destructans* detection (YSW; years 1–4 as a continuous variable) as population-level effects. The response variable was the detection of the fungus, *P. destructans* in each sample determined by qPCR. Each sample is a Bernoulli trial with a 1 indicating a positive detection, and 0 indicating no detection of *P. destructans*. The model is parameterized in relation to the reference level or intercept (FAR) and each parameter represents the difference from this reference level, incorporating the effect of date, each sample type and year since first pathogen detection. Results can be visualized in Fig. 2A.

	Posterior Mean ± Standard Error (95% CI)
Intercept (Substrate_FAR)	-2.98 ± 0.34 (-3.67,-2.32)
Substrate_NEAR	0.18 ± 0.34 (-0.48,0.89)
Substrate_UNDER	0.84 ± 0.3 (0.26,1.43)
Date	0.13 ± 0.07 (-0.02,0.27)
YSW	1 ± 0.12 (0.77,1.26)
Substrate_NEAR:Date	0.01 ± 0.1 (-0.19,0.19)
Substrate_UNDER:Date	0.06 ± 0.08 (-0.1,0.23)
Substrate_NEAR:YSW	0.03 ± 0.17 (-0.3,0.36)
Substrate_UNDER:YSW	0.16 ± 0.15 (-0.13,0.46)
Date:YSW	-0.02 ± 0.04 (-0.09,0.05)
Substrate_NEAR:Date:YSW	0.09 ± 0.05 (-0.01,0.19)
Substrate_UNDER:Date:YSW	0.1 ± 0.05 (0.01,0.19)

Table S5. Coefficients from a Bayesian hierarchical model for changes in pathogen prevalence in North America on different species in different years since pathogen detection. The data were analyzed with a binomial distribution and logit link including site as a group level effect and date interacting with species (*Myotis lucifugus* (MYLU)*, Eptesicus fuscus* (EPFU)*, Myotis septentrionalis* (MYSE)*, Myotis sodalis* (MYSO) and *Perimyotis subflavus* (PESU)) and year since first *P. destructans* detection (YSW; years 1–4 as a categorical variable) as population-level effects. The response variable was the detection of the fungus, *P. destructans* in each sample determined by qPCR. Each bat sampled is a Bernoulli trial with a 1 indicating a positive detection, and 0 indicating no detection of *P. destructans*. The model is parameterized in relation to the reference level or intercept (MYLU, YSW0) and each parameter represents the difference from this reference level, incorporating the effect of date, each species and year since first pathogen detection. Results can be visualized in Fig. 2B.

	Posterior Mean ± Standard Error (95% CI)
Intercept (MYLU)	-7.79 ± 2.78 (-13.93,-3.07)
Species EPFU	-2.98 ± 3.98 (-10.98,4.61)
Species MYSE	-3.26 ± 3.75 (-11.17,3.52)
Species MYSO	-3.92 ± 4.44 (-12.73,4.46)
Species PESU	-2.82 ± 3.68 (-10.49,3.78)
Date	-5.44 ± 2.83 (-11.41,-0.44)
YSW1	3.16 ± 2.79 (-1.6,9.29)
YSW2	10.22 ± 2.77 (5.5,16.28)
YSW3	11.14 ± 2.78 (6.47,17.21)
YSW4	10.38 ± 2.78 (5.64,16.35)
Species EPFU:Date	-0.77 ± 3.95 (-8.93,6.29)
Species MYSE:Date	1.24 ± 3.73 (-6.63,8.06)
Species MYSO:Date	2.85 ± 4.39 (-5.73,11.43)
Species PESU:Date	-0.54 ± 3.8 (-8.44,6.41)
Species EPFU:YSW1	2.25 ± 4.15 (-5.69,10.68)
Species MYSE:YSW1	2.46 ± 3.81 (-4.55,10.41)
Species MYSO:YSW1	2.59 ± 4.6 (-6.27,11.59)
Species PESU:YSW1	2.1 ± 3.74 (-4.72,10)
Species EPFU:YSW2	0.5 ± 3.98 (-7.11,8.52)
Species MYSE:YSW2	1.35 ± 3.79 (-5.65,9.25)
Species MYSO:YSW2	-4.66 ± 5.63 (-16.3,6.08)
Species PESU:YSW2	1.14 ± 3.68 (-5.46,8.84)
Species EPFU:YSW3	-0.52 ± 3.98 (-8.11,7.52)
Species MYSE:YSW3	0.77 ± 4.11 (-6.93,9.13)
Species MYSO:YSW3	-0.13 ± 4.92 (-9.72,9.28)
Species PESU:YSW3	0.86 ± 3.71 (-5.82,8.59)
Species EPFU:YSW4	-0.26 ± 4.01 (-7.87,7.83)

	Posterior Mean ± Standard Error (95% CI)
Species MYSE:YSW4	0.91 ± 4.17 (-7.14,9.51)
Species MYSO:YSW4	0.93 ± 4.45 (-7.56,9.73)
Species PESU:YSW4	0.71 ± 3.71 (-5.94,8.36)
Date:YSW1	6.67 ± 2.83 (1.66,12.63)
Date:YSW2	5.76 ± 2.83 (0.77,11.7)
Date:YSW3	5.55 ± 2.83 (0.57,11.53)
Date:YSW4	5.34 ± 2.83 (0.33,11.3)
Species EPFU:Date:YSW1	0.7 ± 3.95 (-6.39,8.91)
Species MYSE:Date:YSW1	-0.9 ± 3.73 (-7.75,6.91)
Species MYSO:Date:YSW1	-2.69 ± 4.4 (-11.28,5.95)
Species PESU:Date:YSW1	0.31 ± 3.8 (-6.62,8.16)
Species EPFU:Date:YSW2	0.97 ± 3.95 (-6.07,9.11)
Species MYSE:Date:YSW2	1.97 ± 3.95 (-5.29,10.26)
Species MYSO:Date:YSW2	7.84 ± 6.82 (-4.21,22.11)
Species PESU:Date:YSW2	0.76 ± 3.8 (-6.11,8.63)
Species EPFU:Date:YSW3	1.29 ± 3.95 (-5.76,9.5)
Species MYSE:Date:YSW3	9.46 ± 7.09 (-3.14,24.38)
Species MYSO:Date:YSW3	2.95 ± 5.55 (-6.96,15.05)
Species PESU:Date:YSW3	1.16 ± 3.8 (-5.78,8.96)
Species EPFU:Date:YSW4	1.46 ± 3.95 (-5.62,9.66)
Species MYSE:Date:YSW4	1.96 ± 4.49 (-5.92,11.46)
Species MYSO:Date:YSW4	-2.03 ± 4.39 (-10.56,6.58)
Species PESU:Date:YSW4	1.48 ± 3.81 (-5.48,9.48)

Table S6. Coefficients from a Bayesian hierarchical model examining the persistence of *P. destructans* in the environmental reservoir over summer in the United States.

The response variable was the detection of the fungus, *P. destructans* in each sample determined by qPCR. Each sample as a Bernoulli trial with a 1 indicating a positive detection, and 0 indicating no detection of *P. destructans*. The data were analyzed with a binomial distribution and logit link including sample type and site as a group level effect and date interacting with year since *P. destructans* invasion as population-level effects. The model is parameterized in relation to the reference level or intercept (Summer 1) and each parameter represents the difference from this reference level. Results can be visualized in Fig. S2A.

	Posterior Mean ± Standard Error (95% CI)
Intercept (US Summer 1)	-2.41 ± 0.81 (-4.02,-0.7)
Summer Date	0.13 ± 0.02 (0.1,0.17)
Summer 2	2.46 ± 0.2 (2.07,2.88)
Summer 3	3.21 ± 0.22 (2.79,3.65)
Summer 4	2.96 ± 0.25 (2.46,3.45)
Date: Summer 2	-0.13 ± 0.02 (-0.18,-0.09)
Date:Summer 3	-0.18 ± 0.03 (-0.23,-0.13)
Date:Summer 4	-0.09 ± 0.04 (-0.16,-0.02)

Table S7. Coefficients from a Bayesian hierarchical model examining the change in pathogen loads (log_{10} ng of DNA) between spring and autumn in the environmental reservoir across the globe. The data were analyzed with a gaussian distribution and logit link including site and sample type as a group level effect and season interacting with country as population-level effects. The response variable was the quantity of *P. destructans* DNA in each sample determined by qPCR. The model is parameterized in relation to the reference level or intercept and each parameter represents the difference from this reference level, incorporating the effect of site and type. Results can be visualized in Fig. S2B.

	Posterior Mean ± Standard Error (95% CI)
Intercept (Early hibernation)	-5.82 ± 0.62 (-6.99,-4.6)
Late hibernation	-0.08 ± 0.05 (-0.18,0.02)
China	-1.82 ± 0.5 (-2.78,-0.82)
Hungary	-1.6 ± 0.55 (-2.7,-0.51)
United Kingdom	-1.22 ± 0.54 (-2.29,-0.13)
Late Hiber:China	0.54 ± 0.1 (0.34,0.74)
Late Hiber:Hungary	0.76 ± 0.13 (0.51,1)
Late Hiber:UK	-0.02 ± 0.12 (-0.24,0.22)

Table S8. Coefficients from a Bayesian hierarchical model for changes in pathogen prevalence on different species in North America (invasion and established), Europe and Asia over winter (Fig. 3 country panels). The data were analyzed with a binomial distribution and logit link including site as a group level effect and date interacting with species and country as population-level effects (species list in Table S1). Data from the U.S. were divided into samples collected during the first year of pathogen invasion (year 1) and subsequent years once the pathogen was established in sites (years 2–4). The response variable was the detection of the fungus, *P. destructans* in each sample determined by qPCR. Each sample as a Bernoulli trial with a 1 indicating a positive detection, and 0 indicating no detection of *P. destructans*. The model is parameterized in relation to the reference level or intercept (*Myotis lucifugus*, MYLU (US): Invasion year 1) and each parameter represents the difference from this reference level, incorporating the effect of date, and country. Results visualized in Fig. 3 country panels.

	Posterior Mean ± Standard Error (95% CI)
Intercept (MYLU: Invasion)	-4.67 ± 0.5 (-5.71,-3.75)
Date	1.23 ± 0.11 (1.02,1.46)
Species:country EPFU_Invasion	-0.77 ± 1.49 (-4.21,1.69)
Species:country EPFU_Established	4.29 ± 0.51 (3.37,5.29)
Species:country EPGO_Mongolia	-0.1 ± 9.79 (-19.88,18.87)
Species:country HYAL_China	0.3 ± 1.58 (-3.2,3.02)
Species:country MIFU_Japan	-2.21 ± 1.72 (-5.73,0.99)
Species:country MUHI_Japan	-7.48 ± 6.08 (-21.65,1.36)
Species:country MULE_China	1.18 ± 0.75 (-0.25,2.68)
Species:country MYBL_Hungary	-6.03 ± 5.55 (-18.27,2.67)
Species:country MYDAU_Hungary	-7.41 ± 5.63 (-20.21,1.1)
Species:country MYDAU_UK	2.66 ± 0.96 (0.75,4.52)
Species:country MYFI_China	-10.46 ± 5.75 (-23.01,-1.14)
Species:country MYGRA_Mongolia	5.55 ± 2.5 (0.42,10.19)
Species:country MYLU_Established	7.25 ± 0.49 (6.37,8.24)
Species:country MYMA_China	-5.68 ± 7.83 (-22.27,7.17)
Species:country MYMA_Japan	-0.6 ± 1.46 (-3.54,2.18)
Species:country MYMBA_UK	6.65 ± 1.99 (2.65,10.38)
Species:country MYMYO_Hungary	1.89 ± 1.05 (-0.2,4)
Species:country MYNA_Hungary	4.92 ± 7.98 (-10.82,20.03)
Species:country MYNA_UK	2.55 ± 1.02 (0.54,4.48)
Species:country MYPE_China	1.94 ± 0.91 (0.19,3.77)
Species:country MYPE_Mongolia	-4.5 ± 7.35 (-20.64,8.16)
Species:country MYPI_China	-7.56 ± 3.04 (-13.94,-1.95)
Species:country MYSE_Invasion	-0.75 ± 0.89 (-2.6,0.9)
Species:country MYSE_Established	5.67 ± 0.7 (4.31,7.01)
Species:country MYSO_Invasion	-1.24 ± 1.61 (-4.89,1.37)

	Posterior Mean ± Standard Error (95% CI)
Species:country MYSO_Established	4.88 ± 0.53 (3.93,5.97)
Species:country PESU_Invasion	-0.72 ± 0.72 (-2.22,0.61)
Species:country PESU_Established	5.53 ± 0.49 (4.64,6.5)
Species:country PLOG_China	-2.44 ± 4.14 (-12.33,3.72)
Species:country PLOG_Mongolia	-2.01 ± 3.5 (-9.35,4.24)
Species:country RHCO_Japan	0.61 ± 1.22 (-1.84,2.94)
Species:country RHFE_China	1.29 ± 0.67 (-0.04,2.64)
Species:country RHFE_Hungary	1.21 ± 1.56 (-2.04,4.08)
Species:country RHFE_Japan	0.61 ± 0.92 (-1.23,2.38)
Species:country RHFE_UK	-0.71 ± 1.6 (-3.9,2.39)
Species:country RHHI_Hungary	0.97 ± 1.27 (-1.63,3.38)
Species:country RHPU_China	-2.42 ± 2.41 (-7.19,2.04)
Date:Species:country EPFU_Invasion	-0.06 ± 0.34 (-0.62,0.71)
Date:Species:country EPFU_Established	-0.61 ± 0.13 (-0.87,-0.36)
Date:Species:country EPGO_Mongolia	-0.5 ± 1.8 (-4.04,3.15)
Date:Species:country HYAL_China	-0.79 ± 0.46 (-1.7,0.11)
Date:Species:country MIFU_Japan	0.59 ± 0.46 (-0.25,1.55)
Date:Species:country MUHI_Japan	1.09 ± 1.16 (-0.61,3.79)
Date:Species:country MULE_China	-0.34 ± 0.14 (-0.62,-0.07)
Date:Species:country MYBL_Hungary	5.87 ± 3.55 (0.44,13.77)
Date:Species:country MYDAU_Hungary	5.13 ± 3.57 (0.17,13.31)
Date:Species:country MYDAU_UK	-0.44 ± 0.26 (-0.94,0.08)
Date:Species:country MYFI_China	3.04 ± 1.95 (0.05,7.47)
Date:Species:country MYGRA_Mongolia	-0.85 ± 0.54 (-1.82,0.3)
Date:Species:country MYLU_Established	-1.05 ± 0.13 (-1.31,-0.82)
Date:Species:country MYMA_China	1.65 ± 1.59 (-1.05,4.96)
Date:Species:country MYMA_Japan	0.08 ± 0.35 (-0.59,0.81)
Date:Species:country MYMBA_UK	-2.02 ± 0.68 (-3.34,-0.69)
Date:Species:country MYMYO_Hungary	0.14 ± 0.31 (-0.41,0.84)
Date:Species:country MYNA_Hungary	-2.26 ± 5.77 (-13.3,8.9)
Date:Species:country MYNA_UK	-0.44 ± 0.27 (-0.96,0.08)
Date:Species:country MYPE_China	-0.12 ± 0.22 (-0.55,0.32)
Date:Species:country MYPE_Mongolia	2.02 ± 1.96 (-1.22,6.43)
Date:Species:country MYPI_China	1.25 ± 0.71 (-0.06,2.78)
Date:Species:country MYSE_Invasion	0.33 ± 0.22 (-0.07,0.78)
Date:Species:country MYSE_Established	1.56 ± 1.22 (-0.39,4.2)
Date:Species:country MYSO_Invasion	0.15 ± 0.37 (-0.48,0.96)
Date:Species:country MYSO_Established	-0.46 ± 0.16 (-0.79,-0.13)

	Posterior Mean ± Standard Error (95% CI)
Date:Species:country PESU_Invasion	-0.22 ± 0.17 (-0.54,0.13)
Date:Species:country PESU_Established	-0.64 ± 0.13 (-0.91,-0.39)
Date:Species:country PLOG_China	0.14 ± 1.04 (-1.79,2.44)
Date:Species:country PLOG_Mongolia	0.17 ± 0.74 (-1.17,1.73)
Date:Species:country RHCO_Japan	-0.78 ± 0.29 (-1.35,-0.19)
Date:Species:country RHFE_China	-0.41 ± 0.13 (-0.67,-0.17)
Date:Species:country RHFE_Hungary	-0.6 ± 0.35 (-1.25,0.12)
Date:Species:country RHFE_Japan	-0.61 ± 0.18 (-0.96,-0.25)
Date:Species:country RHFE_UK	0.71 ± 0.49 (-0.22,1.71)
Date:Species:country RHHI_Hungary	-0.83 ± 0.28 (-1.36,-0.27)
Date:Species:country RHPU_China	0.22 ± 0.6 (-0.96,1.4)

Table S9. Coefficients from a Bayesian hierarchical model for changes in pathogen prevalence in Israel and Georgia on different species of bats and in the environment (Fig. 3 country panels). Each country was analyzed separately data with a binomial distribution and logit link including site as a group level effect and species (*Rhinolophus ferrumequinum* (RHFE)*, Miniopterus schreibersii* (MISH)*, Myotis capaccinii* (MYCA), *Myotis nattereri* (MYNA)*, Rhinopoma cystops* (RHCY)*, Rhinopoma microphyllum* (RHMI), *Rhinolophus euryale (*RHEU*), Rhinolophus hipposideros* (RHHI), and *Rousettus aegyptiacus* (ROAE)) as a population-level effect. Substrate samples (Under and Near) were included as a level in "species" for comparison in the same analysis. The response variable was the detection of the fungus, *P. destructans* in each sample determined by qPCR. Each sample served as a Bernoulli trial with a 1 indicating a positive detection, and 0 indicating no detection of *P. destructans*. The model is parameterized in relation to the reference level or intercept (RHFE in both countries) and each parameter represents the difference from this reference level for a specific country. Results visualized in Fig. 3 country panels.

	Posterior Mean ± Standard Error (95% CI)
Israel Intercept (RHFE)	-13.46 ± 5.51 (-28.83,-5.87)
Israel: MISH	-1.04 ± 4.46 (-10.58,7.08)
Israel: MYCA	6.2 ± 3.35 (-0.02,13.06)
Israel: MYNA	-0.82 ± 4.56 (-10.03,7.76)
Israel: RHCY	-0.46 ± 4.71 (-10.02,8.65)
Israel: RHEU	-0.83 ± 4.58 (-10.25,7.59)
Israel: RHHI	-0.63 ± 4.62 (-9.87,8.09)
Israel: RHMI	-0.44 ± 4.56 (-9.78,8.12)
Israel: ROAE	-0.59 ± 4.58 (-9.87,7.97)
Israel: Substrate	-0.67 ± 4.05 (-8.82,7.05)
Georgia Intercept (RHFE)	-8.93 ± 5.25 (-20.14,0.5)
Georgia: MISH	8.95 ± 4.51 (1.39,18.9)
Georgia: RHEU	3.7 ± 5.96 (-8.45,15.68)
Georgia: RHHI	4.18 ± 3.76 (-1.99,12.82)

Table S10. Coefficients from a Bayesian hierarchical model for changes in environmental pathogen prevalence over the summer in North America, Europe and Asia. The response variable was the detection of the fungus, *P. destructans* in each sample determined by qPCR. Each sample as a Bernoulli trial with a 1 indicating a positive detection, and 0 indicating no detection of *P. destructans*. The data were analyzed with a binomial distribution and logit link including sample type, site, and year collected as a group level effect and date interacting with country as population-level effects. Data from the U.S. is combined in this analysis and the different years are broken down in Table S8. The model is parameterized in relation to the reference level or intercept (US) and each parameter represents the difference from this reference level, incorporating the effect of date, and country. Results can be visualized in Fig. 4A.

	Posterior Mean ± Standard Error (95% CI)
Intercept (US)	0.06 ± 0.78 (-1.48,1.61)
Summer Date	0.03 ± 0.01 (0.01,0.05)
China	-0.87 ± 0.76 (-2.37,0.66)
Hungary	-0.27 ± 0.86 (-1.98,1.44)
UK	0.09 ± 0.97 (-1.7,2.25)
Summer Date: China	-0.17 ± 0.02 (-0.21,-0.13)
Summer Date: Hungary	-0.19 ± 0.03 (-0.26,-0.14)
Summer Date: UK	-0.21 ± 0.1 (-0.45,-0.04)

Table S11. Coefficients from a Bayesian hierarchical summary model for changes in bat pathogen prevalence in North America (invasion and established), Europe and Asia over winter. The data were analyzed with a binomial distribution and logit link including site and species as a group level effect and date interacting with country as population-level effects. Data from the U.S. was divided into samples collected during the first year of pathogen invasion (US Invasion: year 1) and subsequent years once the pathogen was established in sites (US Established: years 2–4). The response variable was the detection of the fungus, *P. destructans* in each sample determined by qPCR. Each sample as a Bernoulli trial with a 1 indicating a positive detection, and 0 indicating no detection of *P. destructans*. The model is parameterized in relation to the reference level or intercept (United States: Invasion year 1) and each parameter represents the difference from this reference level, incorporating the effect of date, and country. Results can be visualized in Fig. 4B.

	Posterior Mean ± Standard Error (95% CI)
Intercept (US Invasion)	-5.19 ± 0.73 (-6.59,-3.78)
Date	1.2 ± 0.08 (1.05,1.36)
US Established	6.54 ± 0.36 (5.86,7.29)
China	1.84 ± 0.91 (0.01,3.64)
Hungary	1.65 ± 1.11 (-0.59,3.77)
Japan	-0.11 ± 1.06 (-2.22,1.95)
Mongolia	3 ± 2 (-0.88,6.96)
UK	3.08 ± 1.04 (1.01,5.09)
Date: US Established	-0.75 ± 0.09 (-0.93,-0.58)
Date: China	-0.33 ± 0.09 (-0.51,-0.15)
Date: Hungary	-0.33 ± 0.16 (-0.64,-0.02)
Date: Japan	-0.25 ± 0.14 (-0.53,0.04)
Date: Mongolia	-0.6 ± 0.36 (-1.3,0.11)
Date: UK	-0.48 ± 0.18 (-0.84,-0.13)

Table S12. Coefficients from a Bayesian hierarchical model for changes in pathogen loads (log_{10} ng of DNA) on different species in North America (invasion and established), Europe and Asia over winter (Fig. S4). The data were analyzed with a gaussian distribution and logit link including site as a group level effect and date interacting with species and country as population-level effects (species list in Table S1). Data from the U.S. were divided into samples collected during the first year of pathogen invasion (year 1) and subsequent years once the pathogen was established in sites (years 2–4). The response variable was the quantity of *P. destructans* DNA in each sample determined by qPCR. The model is parameterized in relation to the reference level or intercept (*Myotis lucifugus*, MYLU (US): Invasion year 1) and each parameter represents the difference from this reference level, incorporating the effect of date, and country. The posterior mean was extracted from these lines in late winter (March 1st) and are shown in Fig. S4.

	Posterior Mean ± Standard Error (95% CI)
Intercept (MYLU_US Invasion)	-6.66 ± 0.39 (-7.44,-5.91)
Date slope	0.81 ± 0.09 (0.64,0.98)
EPFU_US Invasion	3.02 ± 1.08 (0.87,5.08)
EPFU_US Established	2.03 ± 0.41 (1.25,2.84)
EPGO_Mongolia	0.3 ± 9.9 (-18.41,20.14)
HYAL_China	1.77 ± 1.14 (-0.5,4.07)
MIFU_Japan	-0.2 ± 1.21 (-2.56,2.13)
MUHI_Japan	-0.05 ± 9.79 (-19.73,18.55)
MULE_China	0.5 ± 0.53 (-0.53,1.54)
MYBL_Hungary	0.59 ± 0.86 (-1.1,2.26)
MYDAU_Hungary	1.81 ± 1.74 (-1.78,5.26)
MYDAU_UK	2.4 ± 0.57 (1.27,3.54)
MYFI_China	0.11 ± 2.66 (-5.17,5.38)
MYGRA_Mongolia	3.02 ± 1.11 (0.76,5.24)
MYLU_US Established	3.38 ± 0.39 (2.64,4.14)
MYMA_China	3.15 ± 7.74 (-12.31,18.21)
MYMA_Japan	1.6 ± 1.21 (-0.72,3.98)
MYMBA_UK	2.19 ± 1.45 (-0.63,5)
MYMYO_Hungary	2.4 ± 0.65 (1.12,3.65)
MYNA_UK	1.29 ± 0.69 (-0.03,2.68)
MYPE_China	0.72 ± 0.61 (-0.46,1.88)
MYPE_Mongolia	1.24 ± 1.79 (-2.28,4.73)
MYPI_China	-0.86 ± 1.77 (-4.41,2.52)
MYSE_US Invasion	1.5 ± 0.73 (0.03,2.89)
MYSE_US Established	3.44 ± 0.41 (2.66,4.23)
MYSO_US Invasion	1.78 ± 1.19 (-0.46,4.16)
MYSO_US Established	1.94 ± 0.42 (1.17,2.76)

	Posterior Mean ± Standard Error (95% CI)
PESU_US Invasion	1.27 ± 0.63 (0.04,2.48)
PESU_US Established	3.2 ± 0.39 (2.46,3.96)
PLOG_China	0.15 ± 9.66 (-18.82,19.65)
PLOG_Mongolia	-3.38 ± 2.54 (-8.28,1.71)
RHCO_Japan	-0.26 ± 1.08 (-2.36,1.84)
RHFE_China	0.51 ± 0.47 (-0.4,1.41)
RHFE_Hungary	0.72 ± 1.36 (-1.87,3.43)
RHFE_Japan	0 ± 0.74 (-1.43,1.43)
RHFE_UK	0.19 ± 1.14 (-2.09,2.46)
RHHI_Hungary	0.82 ± 0.99 (-1.17,2.79)
RHPU_China	-0.46 ± 1.76 (-3.92,2.92)
Date:EPFU_US Invasion	-0.97 ± 0.24 (-1.44,-0.49)
Date:EPFU_US Established	-0.48 ± 0.1 (-0.66,-0.3)
Date:EPGO_Mongolia	-0.6 ± 1.81 (-4.16,2.78)
Date:HYAL_China	-0.9 ± 0.38 (-1.63,-0.15)
Date:MIFU_Japan	-0.43 ± 0.25 (-0.91,0.05)
Date:MUHI_Japan	-0.36 ± 1.86 (-3.91,3.38)
Date:MULE_China	-0.43 ± 0.11 (-0.65,-0.21)
Date:MYBL_Hungary	-0.01 ± 0.2 (-0.39,0.41)
Date:MYDAU_Hungary	-0.78 ± 0.42 (-1.59,0.09)
Date:MYDAU_UK	-0.85 ± 0.15 (-1.15,-0.55)
Date:MYFI_China	-0.41 ± 0.63 (-1.66,0.8)
Date:MYGRA_Mongolia	-0.91 ± 0.21 (-1.33,-0.51)
Date:MYLU_US Established	-0.34 ± 0.09 (-0.51,-0.17)
Date:MYMA_China	-0.71 ± 1.53 (-3.68,2.32)
Date:MYMA_Japan	-0.62 ± 0.25 (-1.1,-0.15)
Date:MYMBA_UK	-0.86 ± 0.51 (-1.89,0.12)
Date:MYMYO_Hungary	-0.46 ± 0.14 (-0.73,-0.17)
Date:MYNA_UK	-0.45 ± 0.19 (-0.84,-0.09)
Date:MYPE_China	-0.21 ± 0.13 (-0.45,0.04)
Date:MYPE_Mongolia	-0.32 ± 0.35 (-1,0.36)
Date:MYPI_China	-0.47 ± 0.37 (-1.2,0.28)
Date:MYSE_US Invasion	-0.17 ± 0.16 (-0.49,0.15)
Date:MYSE_US Established	-0.3 ± 0.1 (-0.51,-0.1)
Date:MYSO_US Invasion	-0.6 ± 0.25 (-1.1,-0.11)
Date:MYSO_US Established	-0.47 ± 0.1 (-0.66,-0.28)
Date:PESU_US Invasion	-0.25 ± 0.14 (-0.52,0.02)
Date:PESU_US Established	-0.43 ± 0.09 (-0.61,-0.25)

	Posterior Mean ± Standard Error (95% CI)
Date:PLOG_China	-0.17 ± 2.57 (-5.28,5)
Date:PLOG_Mongolia	0.43 ± 0.53 (-0.61,1.45)
Date:RHCO_Japan	-0.3 ± 0.28 (-0.85,0.25)
Date:RHFE_China	-0.53 ± 0.1 (-0.72,-0.34)
Date:RHFE_Hungary	-0.7 ± 0.31 (-1.32,-0.1)
Date:RHFE_Japan	-0.54 ± 0.15 (-0.84,-0.24)
Date:RHFE_UK	-0.56 ± 0.36 (-1.28,0.16)
Date:RHHI_Hungary	-0.78 ± 0.23 (-1.24,-0.31)
Date:RHPU_China	-0.63 ± 0.44 (-1.47,0.22)

Table S13. Coefficients from a Bayesian hierarchical model examining bat roosting temperatures across North America, Europe and Asia. The data were analyzed with a normal distribution, including site and species as a group level effect and country as a population-level effect. The model is parameterized in relation to the reference level or intercept (United States) and each parameter represents the difference from this reference level. Results can be visualized in Fig. S13.

	Posterior Mean ± Standard Error (95% CI)
Intercept (US)	7.92 ± 0.49 (6.96,8.9)
China	-0.78 ± 0.71 (-2.16,0.63)
Georgia	0.71 ± 1.22 (-1.68,3.06)
Hungary	0.31 ± 0.94 (-1.57,2.11)
Israel	6.67 ± 1.1 (4.55,8.88)
Japan	0.83 ± 0.78 (-0.71,2.37)
Mongolia	-6.49 ± 1.11 (-8.61,-4.13)
United Kingdom	-3.08 ± 0.84 (-4.72,-1.45)

Table S14. Coefficients from a Bayesian hierarchical model examining colony size across North America, Europe and Asia. The data were analyzed with a normal distribution, including country as a group level effect and site and species as a population-level effect. The model is parameterized in relation to the reference level or intercept (China) and each parameter represents the difference from this reference level. Results can be visualized in Fig. S14.

	Posterior Mean ± Standard Error (95% CI)
Intercept (China)	2.03 ± 0.17 (1.69,2.35)
Georgia	0.55 ± 0.39 (-0.19,1.32)
Hungary	-0.42 ± 0.29 (-0.98,0.13)
Japan	0.37 ± 0.29 (-0.17,0.97)
Mongolia	-0.91 ± 0.34 (-1.56,-0.26)
United Kingdom	-0.52 ± 0.23 (-0.97,-0.06)
U.S. Pre-establishment	-0.04 ± 0.2 (-0.43,0.37)
U.S. Established	-0.53 ± 0.2 (-0.92,-0.13)